Energetics of antiphase boundaries in GaAs

David Vanderbilt
Department of Physics and Astronomy, Rutgers University, Piscataway, New Jersey 08855-0849

Changyol Lee
Department of Physics, Harvard University, Cambridge, Massachusetts 02138
(Received 4 November 1991)

Structural energies of antiphase boundaries in GaAs are studied theoretically using a pseudopotential density-functional approach. The formation energy is calculated for several antiphase boundaries having different orientation and stoichiometry. The lowest-energy (110) and (001) boundaries are predicted to be stoichiometric (having no net excess of As or Ga atoms at the interface), while the (111) antiphase boundary is predicted to be nonstoichiometric. The (110) boundary has the lowest formation energy per unit area of those studied. Simple models of the energetics are discussed and compared with the first-principles results. Simple wrong-bond counting is found to be grossly inadequate. An extended model of pair interactions involving a Madelung sum for distant neighbors is formulated and found to give a reasonable description of stoichiometric antiphase boundaries. Nonstoichiometric antiphase boundaries require special treatment, as they generally have a partially filled donor or acceptor band and should be treated as metallic.

I. INTRODUCTION

In recent years there has been growing interest in the electronic and structural properties of antiphase boundaries (APB's) in GaAs and other III-V compounds. An APB is a planar topological defect across which there is a reversal of the assignment of cation and anion species to the two sublattices of the zinc-blende crystal.[1,2] Such defects have been imaged by a number of workers using transmission-electron-microscopy (TEM) techniques.[3–5]

APB's commonly occur as a result of heteroepitaxial growth of GaAs on a (001) face of a Si or Ge substrate, and are associated with preexisting single-height steps.[2] The reason for this is illustrated in Fig. 1. On each terrace, the assignment of atomic species to the A and B sublattices is established by the initial attachment of an As monolayer to the Ge substrate. This assignment will be consistent on either side of a double-height step, but will be reversed across a single-height step. Thus, an APB will necessarily grow upwards from every single-height step. Such steps are common, as a result of imperfect miscut of the (001) surface. The resulting APB's are believed to interfere with the electrical properties of the GaAs overlayer. Figure 1 also illustrates some of the low-order orientations that are possible for APB's.

TEM studies have indicated that APB's tend to self-annihilate during the first several hundred angstroms of overlayer growth.[4,5] Several authors have suggested that this could result from an alternation from step to step of the preferred APB orientation.[5–7] For example, Fig. 2 illustrates one mechanism for APB self-annihilation, which relies on the assumption that APB's oriented along {111} directions are energetically favored. Then for a step along $\langle 1\bar{1}0\rangle$ as shown, the APB can grow up in either the (111) or $(11\bar{1})$ orientation. But these two orientations are not equivalent, as is evident from the figure; one results in an As-rich APB, and the other in a Ga-rich one. Moreover, the assignment of type (As-rich or Ga-rich) to orientation reverses itself for each consecutive single-height step. Thus, no matter whether it is the Ga-rich or As-rich APB which is favored, the orientation of the APB's emitted from the steps will alternate from step to step. Consequently, the APB's will annihilate within a distance to

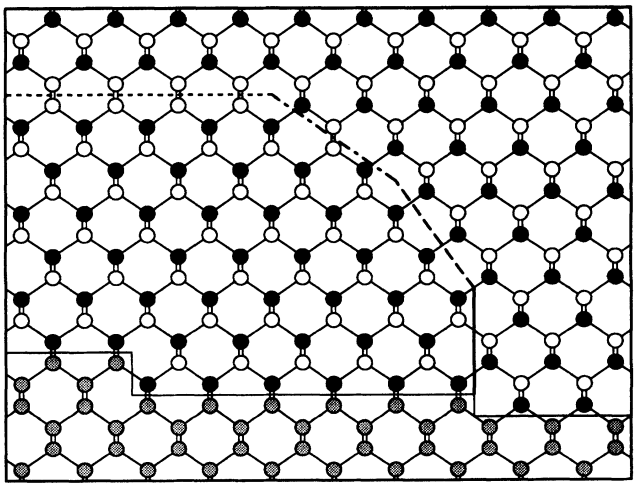

FIG. 1. APB's of several different orientations in a GaAs film grown on Ge (001). Light, medium, and dark filled circles represent Ga, Ge, and As, respectively. Heavy solid, dashed, dashed-dotted, and dotted lines represent (110), (111), (112), and (001) APB's, respectively. The light solid line indicates interface position; the APB emerges from a single-height step, but not from a double-height step.

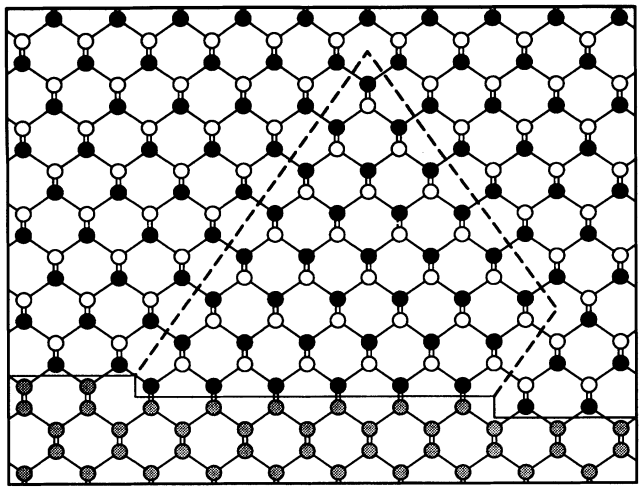

FIG. 2. As in Fig. 1, but showing a model for self-annihilation of APB's via preferential formation of As-rich APB's in the {111} orientations.

the interface, which is comparable to the step-step separation, and the remainder of the heteroepitaxial film will be APB free.

Unfortunately there is little evidence to support the assumption that APB's in the (111) orientation are preferred, as required by the above scenario. In fact, TEM observations[3] suggest that the (110) orientation is most common, followed by (100). Thus, the above scenario will require some revision.

Clearly, an understanding of the electronic and structural properties of APB's, and especially of their formation energy as a function of orientation, is highly desirable. Previous estimates of the energetics of APB's, based on wrong-bond counting models, will be shown to be seriously inadequate. The primary purpose of the present work is to carry out realistic calculations of the energies of APB's of differing orientation, stoichiometry, and local structure. We will also discuss attempts to develop more realistic models for the energetics which can do a reasonable job of reproducing the calculated energies.

In this work, we restrict ourselves to APB structures in which the diamond lattice remains intact. We have not attempted to estimate the energies of APB structures containing vacancies, interstitials, dislocations, or other crystal defects. Thus, the only degrees of freedom in our problem are the assignment of species to each atom in the diamond lattice, and any small (harmonic) lattice relaxations which may result. For the most part we believe that such defects would only be likely to raise the APB energy, and would therefore occur only rarely in an intrinsic APB structure. An important exception is the possible occurrence of relaxations of the type predicted by Chadi and Chang[12] and Zhang and Chadi[13] for As and Ga antisites in GaAs. These are broken-bond configurations in which one or both atoms attached to a wrong bond undergo substantial displacements away from one another; they may be stable or low-energy excited metastable configurations, depending upon details of the defect and charge state. Such structures could very well occur for some APB's, e.g., the Ga-rich (111) APB. This is a natural avenue for future exploration.

The manuscript is organized as follows. In Sec. II we discuss possible interface geometries for APB's in the (001), (011), and (111) orientations, and consider the counting of wrong bonds and excess stoichiometry at the APB. Section III introduces several possible models for the energetics of such APB's. In Sec. IV we present our method of calculation and our numerical results. The extrapolation of these supercell results to the relevant case of distant APB's, and the consequences of the results for models of APB annihilation and of APB energetics, will be discussed in Sec. V. In Sec. VI we obtain a deeper understanding of attempts to model the APB energies in terms of a two-body Ising-type model; to do so, we carry out a perturbation expansion of the energy as a function of species on each site, treating the species as a continuous parameter. Finally, we summarize with some general conclusions in Sec. VII.

II. INTERFACE GEOMETRIES

Figure 1 indicates the structure of ideal APB's of (110), (111), (112), and (001) orientations. It is evident that for the (110) and (112) orientations, there are equal numbers of Ga-Ga and As-As wrong bonds crossing the interface, so there is no net excess of Ga or As atoms associated with the APB. For the (111) and (001) APB's, on the other hand, all of the wrong bonds crossing the boundary are of the same type, leading to a net excess of As or Ga atoms. We shall refer to such an APB as a "polar" or "nonstoichiometric" APB, and will characterize it by a quantity σ_{As} which is defined as the excess number of As atoms per 1×1 interface unit cell. Such an excess will lead to a charged interface which acts like a donor or acceptor layer.[8–10] Thus, σ_{As} is proportional to the areal donor density (or acceptor density if negative). For example, the ideal (111) APB illustrated in Fig. 1 has a net excess of $\frac{1}{2}$ As atom per interface unit cell, and will act electrically like a "δ doping layer" with one donor per every two interface unit cells.

For the purposes of obtaining σ_{As} and the corresponding dipole density D_{As} (see below), it is convenient to use the following counting argument. The APB configuration can be considered to arise from a reference Ge crystal by the addition of an external point charge of $\pm e$ to each Ge nucleus to convert it into an As or Ga atom, respectively. Furthermore, we can imagine dividing up the point charge into four equal charges of $\pm e/4$ and moving them to the midbond positions of the four bonds connected to the atom in question. (This step is permissible for the purposes of the counting argument because it does not change the monopole or dipole moment of the charge configuration.) For a "right bond" (Ga-As bond) these charges cancel, but As-As and Ga-Ga wrong bonds have charges $\pm e/2$ located at their midbond positions, respectively. Thus

$$\sigma_{\mathrm{As}} = \frac{1}{N}\sum_i q_i \tag{1}$$

and

$$D_{\mathrm{As}} = \frac{1}{N}\sum_i q_i \mathbf{r}_i, \tag{2}$$

where the sum is over wrong bonds i in a system with N interface cells, $\mathbf{r}_i$ are the midbond positions, and $q_i = \pm e/2$ for As-As or Ga-Ga bonds, respectively. The dipole density D_{As} is only well defined when σ_{As} vanishes; in this case it will be related (in first-order perturbation) to the discontinuity $\Delta\phi$ in the electrostatic potential across the APB by

$$\Delta\phi = \frac{4\pi D_{\mathrm{As}}}{\epsilon A}, \tag{3}$$

where ϵ is the bulk dielectric constant and A is the interface cell area.

In the case of polar interfaces ($\sigma_{\mathrm{As}} \neq 0$), substitution of some fraction of interface cations by anions (or vice versa) can restore a stoichiometric interface.[8–10] We will refer to an APB of this type as "compensated." It follows from the discussion above that a compensated APB must have an equal number of As-As and Ga-Ga wrong bonds per unit area of boundary.

Tables I and II give the counting of wrong bonds, of σ_{As}, and of D_{As} for some of the possible APB's that are considered in this work. Table I shows that among ideal APB's the (111) appears most favorable from the point of view of simple wrong-bond counting alone, followed by (110), (112), and (001), in order of increasing wrong-bond density. (Note that our values of the wrong-bond densities differ from erroneous values reported previously by Petroff.[11])

However, the fact that the (111) is nonstoichiometric might increase its energy substantially. (We shall see later that this is indeed the case.) Compensated (001) APB's can be generated by reversing the species of half of the atoms in one or the other of the two interface planes (henceforth "type A" and "type B") or one-fourth of both ("hybrid"); a similar approach works for (111) APB's (Table II). However, in the case of the (111) APB, such a substitution increases the number of wrong bonds attached to the reversed site from one to three. Thus, as indicated in Table I, compensation *increases* the density of wrong bonds for the case of the (111) APB, but not for the (001). If we compare wrong-bond density among stoichiometric (compensated) APB's only, we find that the (110) now appears most favorable, followed by (112), (111), and then (001).

In the case of the simplest compensated (001) and (111) APB's (type A or B), the dipole density D_{As} is nonzero. However, with the right choice of layer stoichiometry, it can be made to vanish (hybrid). APB's of type A and B are equivalent (related by mirror symmetry), so they must have the same formation energy. A question then arises as to whether it is the hybrid structure or the type A/B structure which is energetically preferred. If the latter, this would be a case of spontaneous symmetry breaking, in which the APB would

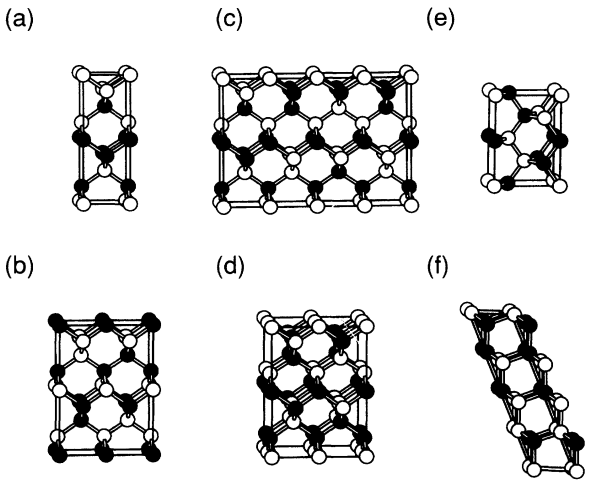

FIG. 3. Supercell structures used for the calculation of APB energies: (a) 1×1 ideal (001) with 8 atoms per cell; (b) 2×1 type A (001) with 16 atoms per cell; (c) 4×1 hybrid (001) with 32 atoms per cell; (d) 2×2 hybrid (001) with 32 atoms per cell; (e) 1×1 ideal (110) with 8 atoms per cell; (f) 1×1 ideal (111) with 8 atoms per cell. Light and dark filled circles represent Ga and As, respectively.

TABLE I. 1×1 interface unit cell (IUC) area, excess stoichiometry σ_{As} per IUC, and nearest-neighbor wrong bonds per IUC and per unit area, for APB's in four different orientations. $a_0 = 5.66$ Å is the GaAs lattice constant; "comp." indicates compensated.

APB orientation and type	IUC area ($\times 4/a_0^2$)	σ_{As} per IUC	Wrong bonds per IUC	Wrong-bond density ($\times a_0^2/4$)
(001) ideal	2	1	2	1.00
(001) comp.	2	0	2	1.00
(110) ideal	$2\sqrt{2}$	0	2	0.71
(111) ideal	$\sqrt{3}$	$\frac{1}{2}$	1	0.58
(111) comp.	$\sqrt{3}$	0	$\frac{3}{2}$	0.87
(112) ideal	$2\sqrt{6}$	0	4	0.82

TABLE II. Ideal and compensated polar APB's. Composition is indicated by giving the layer-by-layer As fraction near the APB; "|" indicates a break between double layers. σ_{As} and D_{As} are the excess As density and dipole density, respectively, per interface unit cell (see the text).

Model	Composition	σ_{As}	D_{As}/a_0
(001) ideal	$\cdots 101101 \cdots$	+1	
(001) type A	$\cdots 10\frac{1}{2}101\cdots$	0	$+\frac{1}{8}$
(001) type B	$\cdots 101\frac{1}{2}01\cdots$	0	$-\frac{1}{8}$
(001) hybrid	$\cdots 10\frac{3}{4}\frac{1}{4}01\cdots$	0	0
(111) ideal	$\cdots\|01\|10\|\cdots$	$+\frac{1}{2}$	
$(\bar{1}\bar{1}\bar{1})$ ideal	$\cdots\|10\|01\|\cdots$	$-\frac{1}{2}$	
(111) type A	$\cdots\|0\frac{3}{4}\|10\|\cdots$	0	$+\sqrt{3}/8$
(111) type B	$\cdots\|01\|\frac{3}{4}0\|\cdots$	0	$-\sqrt{3}/8$
(111) hybrid	$\cdots\|0\frac{7}{8}\|\frac{7}{8}0\|\cdots$	0	0

spontaneously choose one of two directions for the dipole density of the interface. Quite possibly there would be domains of opposite dipole density within a single APB, which would give rise to fringing electric fields. There might also be a critical temperature above which the thermal average of D_{As} vanishes; if so, this would be a novel realization of a 2D Ising transition. We have explored this question for the case of compensated (001) APB's; unfortunately, we find in Sec. IV that the hybrid structure appears to have the lower energy, so that these interesting effects will apparently not occur.

For the purposes of carrying out numerical calculations on the energies of APB's, it is convenient to arrange them into "supercells" which are periodic in all three spatial dimensions. Examples of supercells of this kind are shown in Fig. 3 for several (001), (110), and (111) APB's. Because the regions on either side of an APB are crystallographically distinct, we always have two APB's per supercell. Moreover, in the case of polar APB's, we will choose the excess stoichiometry of the two APB's to cancel, so that there will always be equal numbers of Ga and As atoms in the supercell. In this way, we avoid having to introduce chemical potentials for As and Ga atoms.

III. MODELS FOR ENERGETICS OF ANTIPHASE BOUNDARIES

In this section we discuss possible models for the formation energies of APB's. In Sec. III A we discuss lattice-gas models and their limits of validity. We argue that a model of this kind may be applicable for stoichiometric and compensated APB's (those with $\sigma_{As} = 0$), but cannot possibly be generally valid. We also discuss, in Sec. III B, a rough model for the case of nonstoichiometric APB's, which generally have partially filled donor or acceptor bands and are therefore metallic.

A. Locally stoichiometric APB's

We consider an expansion of the crystal energy of the form

$$E(\{S_i\}) = E_0 + \sum_i H_i S_i + \frac{1}{2!}\sum_{i,j} J_{ij} S_i S_j + \frac{1}{3!}\sum_{i,j,k} K_{ijk} S_i S_j S_k + \cdots, \quad (4)$$

where the degrees of freedom in the problem are the "spin" variables S_i which can take values ± 1 for an As or Ga atom on site i, respectively. By translational symmetry, the linear coefficients H_i must all be equal, and we can take $H_i = \Delta\mu$, the chemical potential difference between As and Ga reservoirs. ($\Delta\mu$ can be ignored for stoichiometric APB's.) Similarly, the $J_{ij} = J(\mathbf{R}_i - \mathbf{R}_j)$ can be interpreted as "exchange couplings" for the spins.

When considered for discrete variables $S_i = \pm 1$, the coefficients appearing in Eq. (4) are not unique. For example, since $S_i^2 = 1$, terms involving diagonal coefficients J_{ii} could be subsumed into E_0. Indeed, alternative expansions are possible and have been successfully used for alloy problems.[14] However, Eq. (4) has the advantage that it can be derived from a perturbation expansion about a virtual crystal state.[15] In this approach, the bare pseudopotential on site i is taken to be

$$V_i = \bar{V} + S_i \Delta V, \quad (5)$$

where $\bar{V}(r) = [V_{As}(r) + V_{Ga}(r)]/2$ is the virtual ion potential, and $\Delta V(r) = [V_{As}(r) - V_{Ga}(r)]/2$ is the perturbing potential. Then the J_{ij} are uniquely defined as the coefficients that arise at second order in the perturbation theory, and could in principle be calculated using linear-response methods.[15] Of course, the perturbation $\Delta V(r)$ used here is stronger and longer ranged than those that have been used for isoelectronic alloys,[14,15] so we cannot be sure *a priori* whether such a perturbation expansion will converge rapidly, or at all, for APB structures of interest. This question will be considered further in Sec. VI, where some numerical tests are carried out.

For many purposes, a simplified empirical version of Eq. (4) would be preferable. A simple counting of wrong bonds, for example, would lead to

$$\Delta E(\{S_i\}) = N_{wb} E_{wb}, \quad (6)$$

where N_{wb} and E_{wb} are the number of wrong bonds and the energy cost for creating them, respectively, and Δ indicates the change relative to an ideal GaAs crystal. Since $N_{wb} = \sum_{\langle ij \rangle}(S_i S_j + 1)/2$, where the sum is over nearest-neighbor pairs $\langle ij \rangle$, Eq. (6) can be considered as a special case of Eq. (4), restricted to nearest-neighbor two-body interactions.

In light of the long range of the perturbing potential $\bar{V}(r)$, the adequacy of a nearest-neighbor expansion is highly dubious. Longer-range two-body interactions can be included approximately by making use of the limiting form $J_{ij} = S_i S_j/\epsilon_0|\mathbf{R}_i - \mathbf{R}_j|$ appropriate for large $|\mathbf{R}_i - \mathbf{R}_j|$. Here ϵ_0 is the static dielectric constant of the virtual crystal. In this case we can write

$$\Delta E(\{S_i\}) = \Delta E_{\rm Mad} + \sum_{m=1}^{M} N_{\rm wb}^{(m)} E_{\rm wb}^{(m)}, \tag{7}$$

where

$$E_{\rm Mad} = \tfrac{1}{2} \sum_{i \neq j} \frac{S_i S_j}{\epsilon_0 |\mathbf{R}_i - \mathbf{R}_j|} \tag{8}$$

is a Madelung sum, and $N_{\rm wb}^{(m)}$ and $E_{\rm wb}^{(m)}$ are the number and energy contribution of mth-neighbor wrong bonds, respectively. (By an mth-neighbor wrong bond, we simply mean a pair of mth-neighbor atoms which are of unlike type if they would normally be of like type, or vice versa. By this definition there are no wrong bonds in ideal GaAs.) Since the sum in Eq. (8) is over all neighbors, $E_{\rm wb}^{(m)}$ is now really the correction to the simple Madelung energy for mth-neighbor bonds. The correction is assumed to be negligible beyond Mth neighbors. The expansion of the form (7) involving first neighbors only ($M = 1$) has actually been suggested long ago by Holt[1] as a natural starting point for APB energetics. As we shall show in Sec. V, we find that Eq. (7) does indeed provide a useful approximation for the formation energies of stoichiometric APB's if corrections up to third neighbor ($M = 3$) are kept.

B. Nonstoichiometric APB's

The lattice-gas expansions given in the preceding subsection cannot possibly be valid generally for nonstoichiometric APB's. For example, consider two ideal (001) APB's, one As-rich and one Ga-rich (with $\sigma_{\rm As} = \pm A\sigma_0$, respectively) separated by a distance L. For large L, this system behaves like two uniform charge sheets of areal charge density σ_0 embedded in a dielectric medium, and therefore contributes an energy per unit area $2\pi L\sigma_0^2/\epsilon_0$ to $E_{\rm Mad}$. Thus, the electrostatic energy diverges linearly with L as the two APB's are pulled apart. Physically, this corresponds to the assumption that the donors or acceptors associated with the nonstoichiometric APB remain fully ionized. However, this assumption breaks down when the electrostatic energy difference across this "parallel plate capacitor" becomes comparable to the energy gap E_g of the semiconductor. At this point it becomes favorable for there to be an electronic charge transfer from one APB to the other; for very large L, a model of neutralized donors and acceptors becomes more appropriate. One cannot expect the perturbation expansion (4) or (7) to "know about" this transition, which involves equilibration of Fermi levels in remote regions. Rather, one should interpret Eq. (4) or (7) as giving the energy for the (possibly nonphysical) case of fully ionized donors and acceptors in the APB's.

To be more quantitative about the argument presented in the preceding paragraph, we consider a periodic array of alternating As-rich and Ga-rich APB's, of separation L, and with fractional ionization f of the donor and acceptor layers associated with the APB's. Thus $f = 0$ and $f = 1$ correspond to fully neutral and fully ionized cases, respectively, and the net free charge on the APB is $\sigma_0 f$. In the limit that σ_0 is small and L is large, we expect the bands to be bent as illustrated in Fig. 4 for the case of intermediate f. The electric field between APB's is $\pm 2\pi\sigma_0 f$, and the resulting energy difference $\Delta\epsilon$ between the donor and acceptor levels on alternating APB's is

$$\Delta\epsilon = E_g - 2\pi L\sigma_0 f/\epsilon_0 \,. \tag{9}$$

If we let E_0 be the energy per unit area per APB pair for the case of fully neutral APB's ($f = 0$), and consider the work done as electrons are transferred from the As-rich to the Ga-rich APB, we obtain

$$E(f) = E_0 - E_g\sigma_0 f + \pi L\sigma_0^2 f^2/\epsilon_0 \,, \tag{10}$$

which is sketched for $f = 0$ and $f = 1$ as the dotted and dashed curves, respectively, in Fig. 5. When E is minimized with respect to f subject to the constraint $f \leq 1$, one obtains

$$f = \begin{cases} 1, & L \leq L_c \\ L_c/L, & L \geq L_c \end{cases} \tag{11}$$

and

$$E_{\rm min} = \begin{cases} E_0 - E_g\sigma_0(1 - L/2L_c), & L \leq L_c \\ E_0 - E_g\sigma_0 L_c/2L, & L \geq L_c, \end{cases} \tag{12}$$

where $L_c = E_g\epsilon_0/2\pi\sigma_0$ is a critical length. For $L < L_c$, the APB's remain fully ionized ($f = 1$), the acceptor levels on the Ga-rich APB nevertheless lie below the donor levels on the As-rich APB's, the system remains insulating, and the expansions (4) and (7) are presumably applicable. For $L > L_c$, on the other hand, the donor and acceptor bands are only partially filled, the APB's become metallic, the Fermi levels of the alternating APB's equilibrate, and the expansions (4) and (7) cannot possibly apply.

Numerous assumptions underlie the above analysis. For example, because energy and position are not simultaneously well defined, Fig. 4 only makes sense for $L \gg a$ (lattice constant). Also, we have assumed that the donor

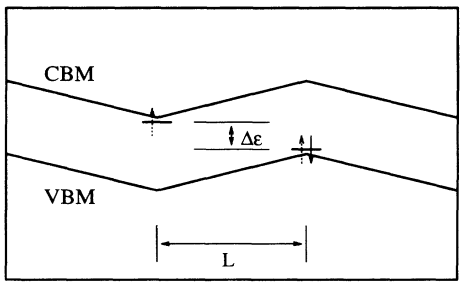

FIG. 4. Sketch of the energy of the conduction-band minimum (CBM) and the valence-band maximum (VBM) as a function of position in the neighborhood of two nonstoichiometric planar APB's of separation L, according to a simple model (see the text). Donor states associated with an As-rich APB on the left are partially ionized, as are acceptor states on a Ga-rich APB at right. $\Delta\epsilon$ is the energy gap between donor and acceptor states.

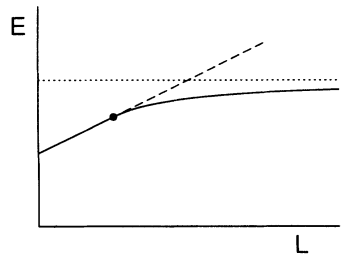

FIG. 5. Creation energy (full line) of a periodic array of alternating As-rich and Ga-rich APB's as a function of separation L, according to a simple model (see the text). The dashed line shows the energy for fully ionized (charged) APB's; the dotted line shows the energy for neutral APB's. The solid dot indicates the critical point separating insulating (left) and metallic (right) APB's, respectively.

and acceptor levels associated with the APB's are shallow; otherwise Eq. (9) needs to be modified. One might also be concerned that the hydrogenic donor or acceptor radius might be large enough to lead to significant overlap. However, the "hydrogenic" states here are really confined in a V-shaped potential (Fig. 4) instead of a $1/r$ potential, and will therefore be much more localized than for an isolated donor or acceptor.

Because of these assumptions, we intend Eq. (12) to be interpreted as merely a rough model which gives a reasonable qualitative description of the crossover between insulating ionized APB's at small L, and nearly neutral metallic APB's at large L. We will also use it in Sec. V to fit our results for the energy of nonstoichiometric APB's as a function of supercell dimension, in order to make an approximate extrapolation to the case of well-separated APB's.

IV. LDA METHODS AND RESULTS

Total-energy calculations were carried out using first-principles norm-conserving pseudopotentials[16] within the framework of the local-density approximation (LDA). Plane waves up to a cutoff of 10 Ry were included exactly using an iterative method for obtaining eigenfunctions of the Schrödinger equation.[17] The charge density was converged using a dielectric matrix as a guide,[18] and using a modified Broyden method[19] to accelerate the convergence. All calculations were carried out using a k-point set corresponding to the 10-k-point set in the irreducible Brillouin zone of the bulk GaAs crystal, thus eliminating systematic errors in comparing energies of different structures.[20] When this bulk 10-point set is folded down to the irreducible Brillouin zone of the APB supercell, we arrive at sets containing between 8 and 30 k points, depending on the supercell dimensions and symmetry.

The results of these total-energy calculations are given in Table III. The results are given relative to the total energy of an equal number of Ga and As atoms in an ideal GaAs crystal. Thus, the energies in Table III can be attributed to the two APB's in the supercell.

In several cases we calculated forces and relaxed the coordinates of the atoms in the supercell, but we found that these relaxation effects were relatively small. For example, for the 8-atom ideal (001) and (111) supercells, the maximum relaxation within the unit cell was found to be about 0.04 Å, and the resulting change of total energy was less than 0.04 eV per supercell. The relaxations for the 8-atom (110) APB were slightly larger, due to reduced symmetry. However, we did not systematically calculate relaxation energies. (Nor have we attempted to calculate the rigid-body translation across the APB, which has recently been measured by Rasmussen, McKernan, and Carter.[21]) Thus, for consistency we have omitted relaxations in all the results quoted in the tables.

V. DISCUSSION

In order to gain insight into these results, we consider some of the models of energetics introduced in Sec. III.

Clearly, the simple wrong-bond counting of Eq. (6) is not an adequate starting point. A comparison of Tables I and III indicates that the interface energy per wrong bond ranges from 0.4 to 0.6 eV, depending on the APB under consideration. Moreover, Eq. (6) would predict that the APB energy should be independent of supercell size, which is clearly not the case for (001) and (111) ideal APB's.

Let us then consider the model of Eq. (7), in which

TABLE III. Calculated and fitted total energy E_{tot} per 1 × 1 interface unit cell per APB pair, relative to ideal GaAs, for supercell structures containing APB's. Asterisks indicate structures that were not included in the fit.

Type	Lateral periodicity	Atoms per supercell	LDA E_{tot} (eV)	Fitted E_{tot} (eV)
(001) ideal	1 × 1	4	1.69	2.42*
(001) ideal	1 × 1	8	2.01	2.79*
(001) type A	2 × 1	16	2.20	2.21
(001) hybrid	2 × 2	32	2.06	1.98
(001) hybrid	4 × 1	32	2.14	2.19
(110) ideal	1 × 1	8	1.58	1.61
(111) ideal	1 × 1	4	0.70	0.69
(111) ideal	1 × 1	8	0.96	0.95*

the energy is expanded in pair interactions which take a simple Madelung form beyond third neighbor. As indicated in Sec. III A, such a model is expected to apply to stoichiometric and compensated APB's. We also expect it to apply to the 4-atom (111) ideal supercell, since in this case the supercell periodicity L is small compared to the critical length L_c, and the APB should remain fully ionized. (Further justification for this statement is given below and in Sec. VI.) For the other polar APB configurations in Table III we expect $L > L_c$, and we do not expect the model to apply.

We have carried out a fit of the model of Eq. (7) to the structures in Table III to which it is expected to apply. The results of the fit are given in the last column of Table III. In the fitting procedure, we fixed $\epsilon_0 = 10$ for the dielectric constant of the virtual crystal (this value was chosen to be close to the known value for Ge), and obtained the values of the three parameters $E_{\rm wb}^{(1)}$, $E_{\rm wb}^{(2)}$, and $E_{\rm wb}^{(3)}$ which gave the best least-squares fit for the five structures indicated in Table III. We found $E_{\rm wb}^{(1)} = 0.463$ eV, $E_{\rm wb}^{(2)} = 0.026$ eV, and $E_{\rm wb}^{(3)} = -0.052$ eV. The good quality of the fit is apparent in Table III. While $E_{\rm wb}^{(2)}$ and $E_{\rm wb}^{(3)}$ may appear small, there are typically ~ 5 times as many second- and third-neighbor wrong bonds as first-neighbor wrong bonds for the APB structures of interest. We found that truncating the sum in Eq. (7) after first or second neighbors (M=1 or 2) resulted in fits of significantly poorer quality.

The fitted values of the APB energies are also reported for the nonstoichiometric APB's (see quantities with asterisks in the last column of Table III). Not surprisingly, the model severely overestimates the energy, at least for the two (001) cases.

Physical APB's in a GaAs crystal will typically be separated by distances much greater than those of any of our superlattice structures. Thus, it is of interest to extrapolate our results to the case of distant APB's. This has been done in Table IV. For the case of stoichiometric APB's, no special extrapolation is necessary; the values in Table IV have been taken directly from the structures with 8 atomic layers per supercell in Table III. This can be justified because the convergence of the energy with respect to supercell dimension is expected to be exponential, with a decay length on the order of the periodicity of the APB structure parallel to the interface. We have tested the dependence of the supercell energy upon repeat distance within the context of the model of Eq. (7), and find that it is already converged to less than 0.02 eV per 1×1 interface cell for the case of an 8-layer supercell.

However, for nonstoichiometric APB's, a more sophisticated extrapolation is necessary. For this purpose, we have applied the model of Sec. III B, which accounts for the crossing of the donor and acceptor levels of distant APB's, and the consequent partial filling of the donor and acceptor bands. We begin by estimating the dimensionless parameter $l = L/L_c$, where L is the APB spacing and $L_c = E_g\epsilon_0/2\pi\sigma_0$ is the critical length defined in Sec. III B. Using $E_g = 1.5$ eV, $\epsilon_0 = 10$, and the values of $\sigma_{\rm As}$ given in Table I, we obtain $l = 1.06$ and 2.13 for ideal (001) APB's in a 4- and 8-atom supercell, respectively. In both cases $l > 1$, so from Eq. (12) we can estimate the energy at infinite separation to be

$$E_0 = E_{\rm LDA} + E_g\sigma_0/2l \ . \tag{13}$$

Putting in numbers, we find $E_0 = 2.40$ and 2.36 for 4- and 8-atom supercells, respectively. For the ideal (111) case, we find in a similar way that $l = 0.71$ and 1.42 for 4- and 8-atom supercells, respectively. Since $l < 1$ for the 4-atom cell, Eq. (12) implies that for this case we should instead use

$$E_0 = E_{\rm LDA} + E_g\sigma_0(1 - l/2) \ . \tag{14}$$

We obtain $E_0 = 1.18$ and 1.22 for 4- and 8-atom (111) supercells, respectively.

The close agreement between the estimates based on 4- and 8-atom cells for both (001) and (111) cases gives us confidence that the rough model of Eq. (12) is adequate for the purpose of extrapolating our results to infinite separation. We have used the values obtained above from the 8-atom cells to derive the final APB energies per unit area given in the first and last row of Table IV. Incidentally, the fact that $l < 1$ for the 4-atom (111) structure justifies the inclusion of this structure in the fit to the model of Eq. (7), as discussed earlier in this section. (Further confirmation of this conclusion is found in Sec. VI.)

For APB's of (001) orientation, note that the compensated APB's of all kinds are preferred over the ideal one. Moreover, the hybrid structures (either 2×2 or 4×1) have a lower energy than the type-A structure. Recall that the former hybrid structures have the dipole density $D_{\rm As} = 0$, while for the latter it is nonzero. If the type-A structure had been found to have the lower energy, this would have suggested a spontaneous symmetry breaking (with respect to the sign of $D_{\rm As}$) and the occurrence of an Ising transition in the equilibrium configuration of the (001) APB as a function of temperature. On the contrary, our results appear to rule out such a possibility. Finally, while the hybrid 2×2 seems to have the lowest energy of (001) APB's, the energy of the 4×1 structure is quite close, and it is quite possible that a disordered configuration, with $D_{\rm As} = 0$ on average, would occur in practice.

Note that the (111) ideal APB energy looks rather low

TABLE IV. Estimated APB creation energy per unit area for distant APB's, as extracted from total-energy calculations. (For nonstoichiometric APB's, the value given is actually the average of the energy of As-rich and Ga-rich versions.)

Type	Lateral periodicity	Creation energy (meV/Å^2)
(001) ideal	1×1	74
(001) type A	2×1	69
(001) hybrid	2×2	64
(001) hybrid	4×1	67
(110) ideal	1×1	35
(111) ideal	1×1	44

in Table III, but when extrapolated to infinite separation, and corrected for unit cell area, the (111) energy becomes substantially higher than for (110). Thus, the ideal (111) APB, which appeared to be the most favorable on the basis of wrong-bond counting alone, is no longer the lowest-energy configuration. While we have not carried out an LDA calculation of the energy of a compensated (111) APB of the kind indicated in Table II, we expect it to have a relatively high energy. This is because compensation requires an increase in the number of wrong bonds in this (111) orientation, as pointed out in Sec. II. We have estimated the energy of a compensated (111) APB using the model of Eq. (7) with the fitted parameters given above; we find an energy of 54 meV/Å, compared to 44 meV/Å for the metallic ideal configuration. Thus, it appears likely that (111) APB's will prefer to remain uncompensated.

If we compare the lowest-energy APB for each orientation, we find that (110) is clearly the preferred orientation, followed by (111), and then (100). Moreover, we find that the energetic advantage of the (110) APB is sufficient to cause faceting of an APB which is initially prepared in a (001) or (111) orientation, provided that such faceting is kinetically allowed. An (001) APB which facets into (011) or (101) orientations increases the APB area by a factor of $\sqrt{2} = 1.41$, but this is less than the ratio 1.83 of the energy per unit area of (001) vs (110) APB's. Similarly, the energy per unit area of the (111) APB exceeds that of the (110) by a factor 1.26, which is slightly larger than the relevant geometric factor of $\sqrt{3/2} = 1.23$. It must be kept in mind, however, that kinetic limitations may prevent such faceting, even when it is energetically favorable.

In Sec. I, we presented a model to explain the tendency for APB's formed during the grown of GaAs on (001) Si or Ge substrates to self-annihilate. That scenario, illustrated in Fig. 2, required APB's of (111) orientation to be energetically preferred. This is at variance with our results, which indicate instead that APB's of (110) orientation will be favored. To explain the experimental indications of self-annihilation, we propose a revised mechanism based on (110) APB's, as illustrated in Fig. 6. Here, we assume that, to a first approximation, APB's grow perpendicular to the substrate with (110) orientation, but that they occasionally have "kinks" or "steps" which shift their position laterally by one lattice unit. Such kinks will either be Ga-rich or As-rich, depending on the direction of the kink; moreover, this dependence upon direction is reversed for alternate APB's (see Fig. 6). If Ga-rich kinks are energetically preferred, alternate APB's will gradually shift in opposite directions until they annihilate. The same is true if As-rich kinks are preferred. In this model, the thickness of the GaAs layer required for self-annihilation is at least several times the step spacing, but otherwise it is similar in spirit to the earlier version based on (111) APB's.

Before closing this section, we wish to emphasize again that our studies have been limited to APB structures in which the bonding of the diamond structure remains intact. As mentioned earlier, broken-bond configurations such as those considered by Zhang and Chadi in the context of point defects[13] have not yet been ruled out. It is possible they could play a role, e.g., for a Ga-rich (111) polar APB. Pending a study of this possibility, we should consider our conclusions that the (110) is energetically favored over (111), and especially that (111) would facet to (110), to be somewhat tentative in nature.

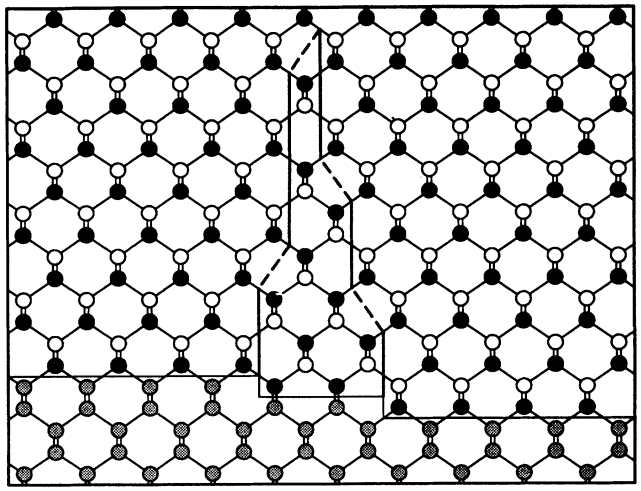

FIG. 6. As in Fig. 1, but showing a revised model for self-annihilation of APB's via preferential formation of As-rich (111) kinks in APB's of (110) orientation.

VI. TREATMENT OF SPECIES AS A CONTINUOUS PARAMETER

In this section, we take a somewhat different approach to understanding the structural energies of the APB's. We replace atoms in the unit cell by imaginary atoms whose properties are a mixture of those of Ga and As. (An approach of this type has been used by Chelikowsky *et al.* to study structural phase transitions as a function of ionicity.[22]) We can represent a given atom in the crystal by a bare pseudopotential which is given by a weighted average of the Ga and As pseudopotentials, as indicated earlier in Eq. (5). We introduce a continuous parameter λ which determines the composition of the atoms in the interface, such that $Ga_{(1+\lambda)/2}As_{(1-\lambda)/2}$ replaces Ga, and $Ga_{(1-\lambda)/2}As_{(1+\lambda)/2}$ replaces As. Thus, the "spin" variables S_i of Eq. (4) now take continuous values $S_i = \pm\lambda$. For $\lambda = 0$, we have an ideal crystal made out of Ge-like atoms, while for $\lambda = 1$ we recover the APB configuration of interest.

We have calculated the energies of several APB configurations as a function of continuous λ using this approach. Results for the energy of ideal (001) and (111) APB's in a 4-atom supercell are shown in Fig. 7. We have plotted $-\Delta E(\lambda)$, where $\Delta E(\lambda) = E(\lambda) - E(0)$. We have also carried out a fit of $-\Delta E(\lambda)$ to a low-order polynomial in λ^2, using the results for $\lambda \leq 0.6$. [For all supercells studied, $E(\lambda)$ is even in λ.] In the ideal (001) APB, we found that $-\Delta E(\lambda)$ visibly deviates from the curve we expect from the expansion in terms of λ^2, while in the ideal (111) APB, $-\Delta E(\lambda)$ follows the expansion

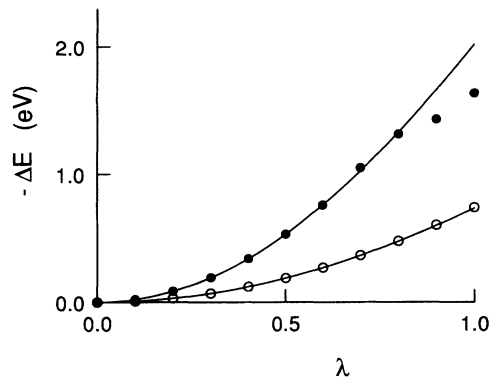

FIG. 7. Plot of $-\Delta E(\lambda)$ vs λ (see the text) for the case of 4-atom supercells of (001) and (111) orientation (filled and open circles, respectively). Solid lines are fourth-order polynomial fits to the calculated values for $\lambda \leq 0.6$.

in terms of λ^2 very well up to $\lambda = 1$. In principle, λ can take any real value, so we increased λ until $-\Delta E(\lambda)$ deviates from the perturbation expansion. We estimate the critical λ_c at which the perturbation theory starts to fail to be around 0.7 and 1.9 for the ideal 4-atom (001) and (111) APB's, respectively.

For polar APB's such as those under consideration, we can understand the breakdown of the perturbation theory following the discussion of the preceding section. When $\lambda = 0$, all the atoms are Ge-like, so there is no spatial dependence of the band structure, and the band bending shown in Fig. 4 is absent. As λ increases, the electric field builds up and the energy bands get tilted. Not until the conduction-band minimum crosses the valence-band maximum ($\lambda \simeq \lambda_c$) does the perturbation expansion break down. In fact, the model predicts $\lambda_c = 1/l$, which would imply λ_c=0.9 and 1.4 for the (001) and (111) 4-atom APB's, respectively. This is in rough agreement with the values obtained empirically above. Thus, both types of analysis lead to a consistent picture, in which the (001) and (111) 4-atom supercells are in the metallic and perturbation regimes, respectively. For the (001) case, partial ionization of interface atoms occurs, the conduction-band minimum equilibrates with the valence-band maximum, and the interface becomes metallic. Meanwhile, for the (111) case, the interface remains fully ionized and insulating. We were therefore justified in including the LDA energy of the ideal (111) APB for a 4-atom supercell in the fitting procedure of Sec. V.

As mentioned earlier, the coefficients at order λ^2 in the perturbation expansion could be calculated efficiently using a linear-response approach.[15] This has not been attempted here. However, such a calculation would be an interesting extension of the present work, particularly if the structural relaxations at harmonic order were simultaneously included using the same linear-response techniques.[15]

VII. SUMMARY AND CONCLUSIONS

We have studied the energies of APB boundaries as a function of orientation, stoichiometry, and local structure. The (110) orientation is found to have the lowest formation energy per unit area, which is consistent with experimental observations indicating that this orientation is the one most frequently observed.

We have argued that approximate models for the energetics of APB's must distinguish between nonstoichiometric ($\sigma_{As} \neq 0$) and stoichiometric ($\sigma_{As} = 0$) configurations. The former are harder to describe properly; we have used a rough band-bending model for this purpose. The latter are amenable to a perturbation approach. Except for APB's of (111) orientation, we find that such stoichiometric structures are always energetically favored over nonstoichiometric ones.

For such stoichiometric APB's, we have proposed a specific model of pair interactions with a long-range Madelung form and near-neighbor corrections through third neighbor, Eq. (7). This model does a reasonable job of reproducing the APB energies calculated within the LDA. One possible avenue for future study would be to use this model to investigate the equilibrium statistical mechanics of the APB configurations at finite temperature, perhaps using Monte Carlo techniques. In this way, one could get statistical averages like layer-by-layer composition (i.e., information about interface width and interdiffusion) and APB free energy as a function of temperature. One could also investigate energies of kinks in APB's. While it is questionable whether equilibration can take place for the temperatures and time scales of experimental interest, such a study would nevertheless provide useful guidance.

Finally, we have discussed mechanisms for the self-annihilation of APB's grown on Si or Ge (001) substrates. Our results suggest that the APB's will primarily grow normal to the substrate in (110) orientation, but we point out that a preference for Ga-rich or As-rich kinks in the APB can indeed provide a tendency toward self-annihilation.

ACKNOWLEDGMENTS

This research was supported by NSF Grant No. DMR-88-17291. D.V. also acknowledges support of the Alfred P. Sloan Foundation. Supercomputer time was provided by the John von Neumann Computer Center, and by the Pittsburgh Supercomputing Center.

[1] D. B. Holt, J. Phys. Chem. Solids **30**, 1297 (1969).
[2] H. Kroemer, J. Cryst. Growth **81**, 193 (1987).
[3] N.-H. Cho *et al.*, Appl. Phys. Lett. **47**, 879 (1985).
[4] O. Ueda, T. Soga, T. Jimbo, and M. Umeno, in *Chemistry and Defects in Semiconductor Heterostructures*, edited by, M. Kawabe, T. D. Sands, E. R. Weber, and R. S. Williams, Materials Research Society Symposia Proceedings No. 148 (MRS, Pittsburgh, 1989), p. 267.
[5] O. Ueda, T. Soga, T. Jimbo, and M. Umeno, Appl. Phys. Lett. **55**, 445 (1989).
[6] M. Kawabe and T. Ueda, Jpn. J. Appl. Phys. **26**, L944 (1987).
[7] J. Varrio *et al.*, Appl. Phys. Lett. **55**, 1987 (1989).
[8] R. W. Nosker, P. Mark, and J. D. Levine, Surf. Sci. **19**, 291 (1970).
[9] P. Masri and M. Lanoo, Surf. Sci. **52**, 377 (1975).
[10] W. A. Harrison, E. A. Kraut, J. R. Waldrop, and R. W. Grant, Phys. Rev. B **18**, 4402 (1978).
[11] P. M. Petroff, J. Vac. Sci. Technol. B **4**, 874 (1986).
[12] D. J. Chadi and K. J. Chang, Phys. Rev. Lett. **60**, 2187 (1988).
[13] S. B. Zhang and D. J. Chadi, Phys. Rev. Lett. **64**, 1789 (1990).
[14] S.-H. Wei and A. Zunger, Phys. Rev. Lett. **61**, 1505 (1988).
[15] S. de Gironcoli, P. Giannozzi, and S. Baroni, Phys. Rev. Lett. **66**, 2116 (1991).
[16] D. Vanderbilt, Phys. Rev. B **32**, 8412 (1985).
[17] R. Natarajan and D. Vanderbilt, J. Comput. Phys. **81**, 218 (1989).
[18] K. M. Ho, J. Ihm, and J. D. Joannopoulos, Phys. Rev. B **25**, 4260 (1982).
[19] D. Vanderbilt and S. G. Louie, Phys. Rev. B **30**, 6118 (1984).
[20] S. Froyen, Phys. Rev. B **39**, 3168 (1989).
[21] D. R. Rasmussen, S. McKernan, and C. B. Carter, Phys. Rev. Lett. **66**, 2629 (1991).
[22] J. R. Chelikowsky and J. K. Burdett, Phys. Rev. Lett. **56**, 961 (1986); J. R. Chelikowsky, Phys. Rev. B **34**, 5295 (1986).

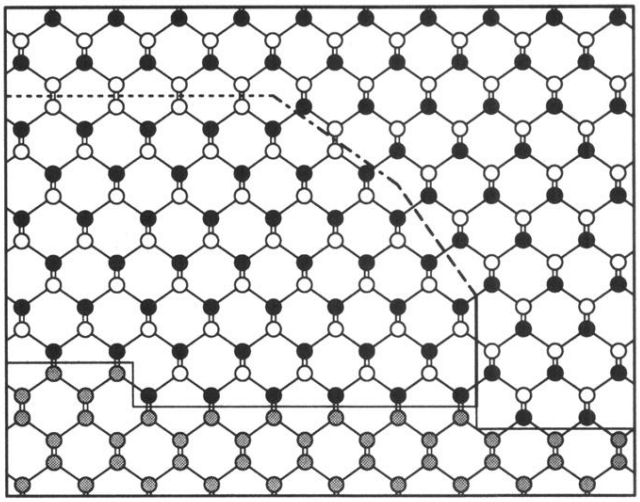

FIG. 1. APB's of several different orientations in a GaAs film grown on Ge (001). Light, medium, and dark filled circles represent Ga, Ge, and As, respectively. Heavy solid, dashed, dashed-dotted, and dotted lines represent (110), (111), (112), and (001) APB's, respectively. The light solid line indicates interface position; the APB emerges from a single-height step, but not from a double-height step.

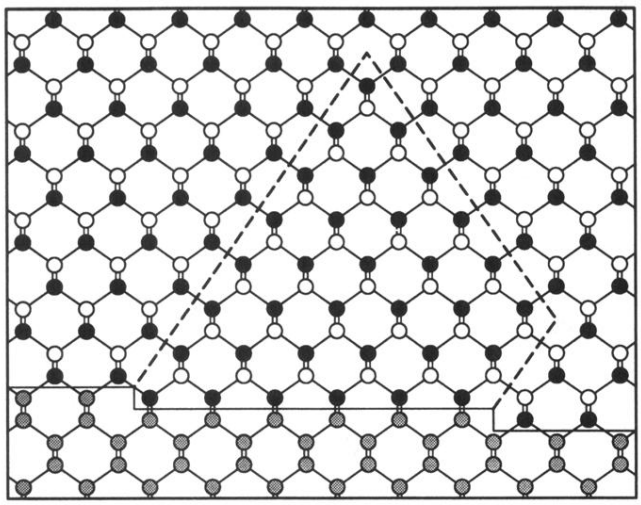

FIG. 2. As in Fig. 1, but showing a model for self-annihilation of APB's via preferential formation of As-rich APB's in the {111} orientations.

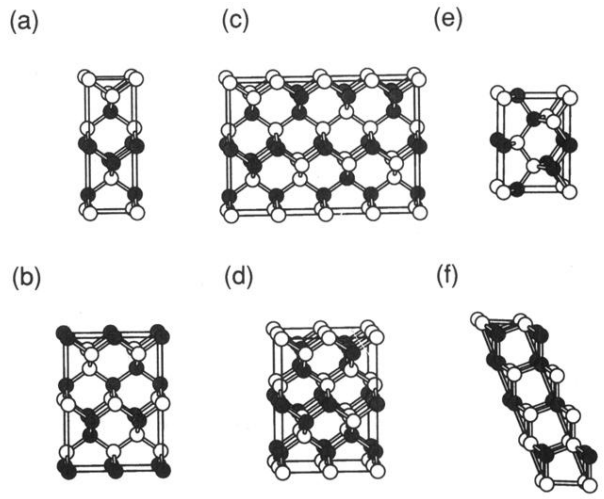

FIG. 3. Supercell structures used for the calculation of APB energies: (a) 1×1 ideal (001) with 8 atoms per cell; (b) 2×1 type A (001) with 16 atoms per cell; (c) 4×1 hybrid (001) with 32 atoms per cell; (d) 2×2 hybrid (001) with 32 atoms per cell; (e) 1×1 ideal (110) with 8 atoms per cell; (f) 1×1 ideal (111) with 8 atoms per cell. Light and dark filled circles represent Ga and As, respectively.

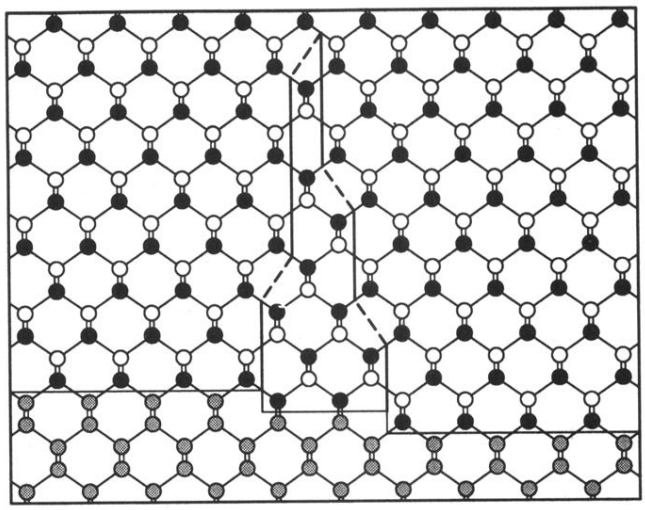

FIG. 6. As in Fig. 1, but showing a revised model for self-annihilation of APB's via preferential formation of As-rich (111) kinks in APB's of (110) orientation.